Dictionary Learning and Waveform Design for Dense False Target Jamming Suppression

Tao Jiang [1], Leixin Yu [1], Jiangnan Xing [1], Yinfeng Xia [1,*], Zhe Du [2], Yingsong Li [1], Guoning Zhi [3], and Yanbo Zhao [3]

[1] College of Information and Communications Engineering
Harbin Engineering University, Harbin, 150001, China
*xiayinfeng@hrbeu.edu.cn

[2] Shanghai Electro-Mechanical Engineering Institute, Shanghai 201109, China

[3] Beijing Aerospace Measurement & Control Technology CO. LTD

Abstract — For linear frequency modulation (LFM) pulse radars, dense false targets generated by new system jamming seriously damage the performance of such radar systems. In order to avoid the influence of dense false target jamming, an anti-jamming strategy combining waveform design and sparse decomposition are proposed. Specifically, the radar system transmits a random pulse initial phase (RPIP) signal, and uses peak detection method to detect the deception jamming. The phase distribution of the RPIP signal is partially randomly perturbed for a jamming, and we use optimization algorithm to design a phase perturbed LFM (PPLFM) signal with good autocorrelation characteristics. Using the correlation function of the designed signal, the target sample set and the jamming sample set are constructed, and the target echo and the jamming signal are separated using designed dictionary learning method to achieve suppression of dense false target jamming and range side-lobes. The effectiveness of the proposed method is verified by numerical simulation, and the results proved that this proposed method maintains good anti-jamming performance under low signal-to-noise ratio (SNR).

Index Terms — Anti-jamming, dense false target jamming, dictionary learning, jamming detection, waveform design.

I. INTRODUCTION

In recent years, the development of radar electronic countermeasures (ECM) technology has made military radars face new challenges. In particular, the rapid development of digital radio frequency memory (DRFM) technology has further promoted the implementation of active deception jamming [1]. Among them, new system jamming such as chopping and interleaving (C&I) and smeared spectrum (SMSP) has the advantages of deception jamming that makes it difficult for LFM radar system to distinguish true or false targets, and saturate radar data processing severely destroys the radar's ability to detect and track targets [2-4].

In response to the influence of sliced jamming (C&I and SMSP), some electronic counter-countermeasures (ECCM) strategies are proposed. Among them, typical methods can be divided into two categories. The first category methods use pulse diversity technology. In [5], a jamming cancellation method based on temporal pulse diversity has been reported for suppressing slice jamming. The waveform design algorithm based on a priori information of electronic jamming in the radar environment knowledge base proposed by [6] achieves suppression of SMSP and C&I jamming. It is worth noting that when there is strong jamming in the radar echo, the higher range side-lobes of the orthogonal signal or quasi-orthogonal signal after matching filtering will still affect the radar's detection performance for real targets. The second category of method is anti-jamming signal processing algorithms. For example, some scholars have used compressed sensing theory and blind source separation technology to achieve the separation of target echo and jamming signals [7, 8]. Paper [9] proposes a countering SMSP jamming method based on jointing time-frequency distribution and compressed sensing. In [10], the authors studied distributed radar to suppress SMSP jamming, and proposed a framework based on joint blind source separation (JBSS). Since noise energy has a great impact on the source method, it makes the jamming suppression performance worse at lower SNR.

In view of the above problems, we consider waveform design to weaken the influence of side-lobes. Since the signal has good sparsity under the adaptive dictionary, we combined the dictionary learning method and sparse decomposition theory to achieve jamming

suppression. Because the agile radar system transmits multiple RPIP signals in a coherent processing interval (CPI), the jammer requires a certain processing time for the radar signal. According to the difference in the initial phase between the jamming signal and the radar emission signal, the proposed peak detection method uses a wavelet transform algorithm to estimate the phase difference of the pulse compression (PC) signal in two adjacent PRIs so as to achieve detection of radar deception jamming. When jamming is detected in the radar echo, the radar system starts to perform phase perturbation processing on the RPIP signal. Then, the integrated auto-correlation side-lobes energy (IASE) of the transmitted signal is minimized as the criterion for waveform design. We use genetic algorithm (GA) to design the parameters of the phase perturbed term and get a series of PPLFM waveforms with good autocorrelation characteristics. In addition, there are many studies on the identification and feature parameter extraction of C&I and SMSP jamming [11, 12]. We assume that the modulation parameters of electronic jamming are known to construct a mathematical model for the jamming signal. Next, the target sample set is constructed using the autocorrelation of the designed PPLFM signal, and the cross correlation between the designed PPLFM signal and the jamming model is used to construct the jamming sample set. Finally, the dictionary learning method proposed in our research work is used to suppress the jamming of dense false targets.

II. SIGNAL MODEL

The RPIP agile waveform is that the radar transmits M-pulse signal with different initial phases in a CPI, and the pulse signal transmitted in the m-th PRI is $S_m(t)$:

$$S_m(t) = e^{j\varphi_m} \cdot s_{LFM}(t) = \exp\left(j\pi\mu t^2 + j\varphi_m\right), \qquad (1)$$

where $\mu = B/T$ is chirp rate, B is pulse bandwidth, T is pulse duration. φ_m is the initial phase of the radar signal, and it follows uniform distribution on $[-\pi, \pi]$.

Assuming that the amplitude and delay of the target echo remain unchanged within a CPI, then, the target echo can be modeled as:

$$T_m(t) = \sigma_T \cdot e^{j\varphi_m} \cdot s_{LFM}(t - \tau_T), \qquad (2)$$

where σ_T and τ_T denote the amplitude and time-delay of the target echo, respectively.

The mathematical model of C&I jamming can be written as:

$$j_m^1(t) = \sum_{l=0}^{L-1} C_m^1\left(t - l\frac{T}{L \cdot n_{c\&i}}\right), \qquad (3)$$

where L and $n_{c\&i}$ represent the sampling interval and the number of sub-pulse repetitions, respectively:

$$C_m^1(t) = S_m(t) \cdot \sum_{i=1}^{n_{c\&i}} rect\left(\frac{t - \tau_b - (i-1)T}{\tau_b}\right), \qquad (4)$$

where $rect(t)$ is rectangular function, τ_b is the sub-pulse width.

The model expression forming the SMSP jamming is given as follows:

$$j_m^2(t) = \sum_{i=1}^{n_{smsp}} C_m^2\left(t - (i-1)\frac{T}{n_{smsp}}\right), \qquad (5)$$

where n_{smsp} is the number of sub-pulse repetitions,

$$C_m^2(t) = \exp\left(j\pi n_{smsp}\mu t^2\right), \quad 0 \le t \le T/n_{smsp}. \qquad (6)$$

Due to the radar transmission signal intercepted by the DRFM jammer is modulated as a jamming signal, it requires a certain processing time. As the agile radar with RPIP waveform is the active side, the jammer becomes the passive side. Then, the jamming signal for the m-th PRI received by the radar can be expressed as:

$$J_m(t) = \sigma_J \cdot e^{j\varphi_{m-I}} j_m^k(t - \tau_J), \quad k = 1, 2, \qquad (7)$$

where I is the number of PRIs for the jamming signal lagging the transmitted signal.

Then, the radar echo signal received by the radar receiver in the m-th PRI is:

$$r_m(t) = T_m(t) + J_m(t) + N_m(t), \qquad (8)$$

where $N_m(t)$ is white Gaussian noise.

Finally, the radar echo $r_m(t)$ is transmitted to a filter with a matching coefficient of $h_m(t) = S_m^*(-t)$. Then, the PC of the m-th radar echo signal after matching filter can be written as:

$$\begin{aligned} y_m(t) &= r_m(t) \otimes h_m(t) \\ &= \sigma_T R_{LFM}(t - \tau_T) + e^{j\phi_n} \cdot \sigma_J R_{LFM,J}(t - \tau_J) + W_m(t) \end{aligned}, \qquad (9)$$

where $\phi_m = \varphi_m - \varphi_{m-I}$ is the phase residual, $W_m(t)$ is white Gaussian noise. $R_{LFM}(t)$ is the autocorrelation function of signal $s_{LFM}(t)$, $R_{LFM,J}(t)$ is the cross-correlation function between signal $s_{LFM}(t)$ and jamming $j_m^k(t)$.

III. JAMMING SUPPRESSION STRATEGY

The strategy proposed in this paper can both realize the detection of deception jamming and suppress the jamming. Figure 1 shows the workflow of the agile LFM radar against slice jamming. First, the radar transmits RPIP agile pulse signals and uses the peak detection method to determine whether there is jamming in the radar echo. If there is no jamming, the radar system directly detects the real target. If there is a jamming, the agile radar changes to transmit a quasi-RPIP (Q-RPIP) signal. Then, according to a certain process, the peak detection method is used to estimate the lagging I value, and the coding sequence of the phase perturbed term in

the jamming signal is obtained. After that, the agile radar changes to transmit a PPLFM signal via optimized design. We perform autocorrelation processing on the optimized signal, and cross-correlation processing between the optimized signal and the jamming signal, and then, the target sample set and the jamming sample set are constructed in a range gate, respectively. Finally, the sample set of the two signals is used to separate the target and the jamming through the dictionary learning method so that the radar can detect the real target.
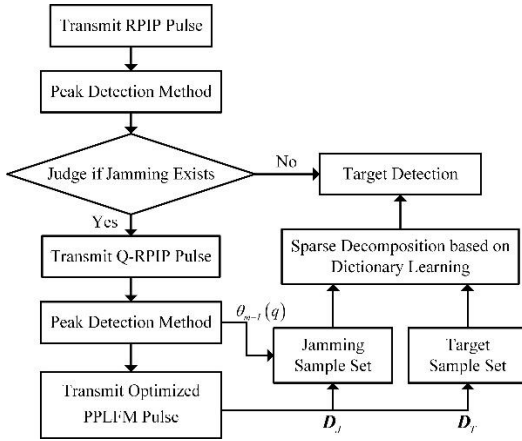
Fig. 1. Agile LFM radar against slice jamming workflow.

A. Detection of deception jamming

This section introduces the basic principle of the peak detection method to detect radar active deception jamming. The radar system transmits the RPIP agile waveform, and the received echo is processed by matched filtering to obtain pulse compression signals $y_m(t)$ and $y_{m+1}(t)$ in the two adjacent PRIs. As shown in Fig. 2, the red dotted line represents SMSP jamming, the blue solid line represents the target echo, and the black dotted line represents noise signal. It is understood from equation (9) that the jamming signal is affected by random initial phase changes, resulting in unequal initial phases of the jamming signals in two adjacent PRIs. In other words, the phase difference of the two jamming signals is non-zero, and the phase difference of the target echo is zero. Therefore, according to this difference characteristic, we intercept the segment of the PC signal with a large peak position and estimate the phase difference of the intercepted signal fragments. If the estimated phase difference is zero, the signal segment is the target signal. If the phase difference is not zero, it means that this signal segment is a jamming signal.

We use the wavelet transform algorithm to estimate the phase difference of the signals in the two adjacent PRIs. According to the definition of wavelet transform, the continuous wavelet transform of signal $s(t)$ is:

$$W_s(a,b) = \frac{1}{\sqrt{a}} \int_{-\infty}^{+\infty} s(t)\Psi^*(\frac{t-b}{a})dt, \qquad (10)$$

where a is scale factor, b is displacement parameters, $*$ represents conjugate, function $\Psi(t)$ is a basic wavelet. In this paper, Morlet wavelet is used as the continuous wavelet transform.
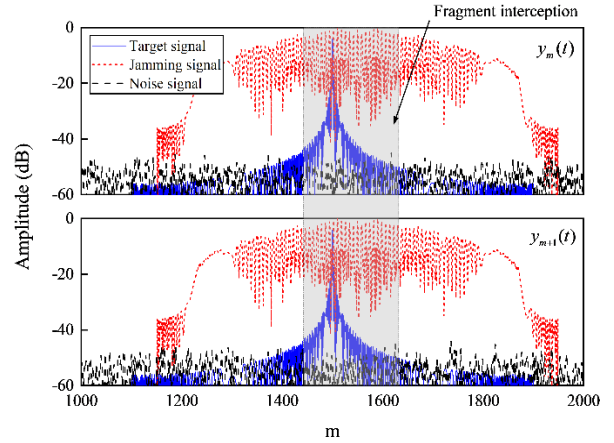
Fig. 2. Schematic diagram of peak detection method.

Intercepting the time series $y'_m(t)$ and $y'_{m+1}(t)$ of the PC signal in the range gate, and defining the cross wavelet transform is given by:

$$W_{y'_m, y'_{m+1}} = W_{y'_m} W^*_{y'_{m+1}}, \qquad (11)$$

where $W_{y'_m}$ and $W_{y'_{m+1}}$ are wavelet transform for $y'_m(t)$ and $y'_{m+1}(t)$, respectively. The corresponding cross wavelet power is $\left| W_{y'_m, y'_{m+1}} \right|$. The estimated phase difference is:

$$\Phi_{y'_m, y'_{m+1}}(a,b) = \arg\left[W_{y'_m, y'_{m+1}}(a,b) \right], \qquad (12)$$

where $\arg[\bullet]$ is used to calculate the complex angle with range of $[-\pi, \pi]$.
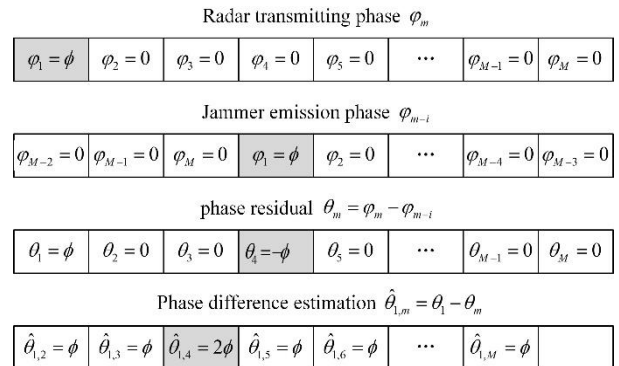
Fig. 3. Schematic of estimated jamming at lagging *I*.

Next, the peak detection method is used to estimate the jamming lagging I. As shown in Fig. 3, the LFM pulse radar transmits the Q-RPIP waveform set. The initial phase of the first signal in the waveform set is set to $\varphi_1 = \phi$, while the initial phase of the other signals is $\varphi_m = 0$ $(m = 2, \cdots, M)$. Assuming that the jamming lagging I is 3, then the initial phase of the fourth pulse signal in the waveform set emitted by the jammer is $\varphi_4 = \phi$. Then, the phase residuals of the first pulse signal and the fourth pulse signal after pulse compression processing are $\theta_1 = \phi$ and $\theta_4 = -\phi$, respectively. Finally, the peak detection method is used to estimate the phase difference between the first PC signal peak and the subsequent M-1 PC signal peaks. The phase difference estimated in the third detection is $\hat{\theta}_{1,3} = 2\phi$, and the other phase differences are estimated to be $\hat{\theta}_{1,m} = \varphi(m \neq 3)$. In this way, it is determined that the number of PRIs for the jamming signal sent by the jammer lagging the transmitted signal is 3.

B. Optimized design of PPLFM waveform

The PPLFM signal constructed using partial random perturbance to the phase distribution of the RPIP signal to get:

$$P_m(t) = S_m(t) \cdot p_m(t)$$
$$= \exp\left(j\pi\mu t^2 + j\theta_m(t) + j\varphi_m \right), \quad (13)$$

where $p_m(t) = \exp\left(j\theta_m(t) \right)$ is the random phase perturbed term in the PPLFM signal.

Generally, random signals $\theta_m(t)$ can be expressed as:

$$\theta_m(t) = \sum_{q=1}^{Q} \theta_m(q) \cdot \left[U\left(t - qt_p\right) - U\left(t - (q-1)t_p\right) \right], \quad (14)$$

where the pulse signal in the time domain is divided into $Q = T/t_p$ sub-pulses, t_p is the width of each sub-pulse in the time domain. $U(t)$ is the step function, $\theta_m(q)$ is the phase coding sequence of the m-th waveform in the waveform set with $\theta_m(q) \in [-\pi, \pi]$.

In order to avoid high range side-lobes jamming, the IASE of the transmitted signal $P_m(t)$ is minimized as basic criterion for waveform design. The calculation of IASE for $P_m(t)$ is:

$$IASE_m = \int_{t \in \text{sidelobe}} \left| R_{P_m}(t) \right|^2 dt, \quad (15)$$

where $R_{P_m}(t)$ is the autocorrelation function of the m-th transmitted signal $P_m(t)$.

According to the above-mentioned waveform design criteria, the waveform design problem model is constructed as follows:

$$\min_{\theta_m} \quad CF = IASE_m. \quad (16)$$

GA is used to solve the optimal solution of the above expressions to minimize the autocorrelation side-lobes energy. The obtained solution is used as the coding sequence of the phase perturbed term.

C. Dictionary learning method to separate target echo and jamming signal

Calculate the autocorrelation function $\bar{R}_{P_m}(t)$ of the optimized PPLFM signal, and construct the target sample set as:

$$D_T = \left\{ D_T^n(t) = \bar{R}_{P_m}\left(t - \tau_n\right), \quad n = 1, 2, \cdots, N \right\}. \quad (17)$$

Then, according to the coding sequence $\theta_{m-I}(q)$ obtained by the peak detection method, the cross-correlation function $\bar{R}_{P_m,J}(t)$ between the jamming signal and the optimized signal is calculated, and the jamming sample set is created as:

$$D_J = \left\{ D_J^n(t) = \bar{R}_{P_m,J}\left(t - \tau_n\right), \quad n = 1, 2, \cdots, N \right\}, \quad (18)$$

where N is the number of all possible echoes within the detection range of the radar range gate. According to the radar range gate width range $\left[d_{\min}, d_{\max} \right]$ and the minimum resolution distance d, the number of atoms in the dictionary is determined as $N = \left(d_{\max} - d_{\min} \right)/d$. Time-delay τ_n can be written as:

$$\tau_n = \frac{2\left(d_{\min} + n \cdot d \right)}{C}, \quad (19)$$

where C is the speed of light.

The atoms in the sample set (initial dictionary) D_T and D_J are converted into autocorrelation matrix diagonal vectors, and then normalized to construct new dictionaries G_T and G_J, respectively. After that, we use the adaptive dictionary learning method to construct the approximate Q-KLT basis of the target and the jamming signal.

The specific steps to achieve the separation of the target echo and the jamming signal under the approximate Q-KLT basis are described below.

(1) Calculate the autocorrelation matrix R_y of the PC signal y in the radar range gate and the diagonal vector d_y.

(2) We use OMP algorithm to iterate the input signal d_y and the joint dictionary $G_{unit} = [G_T, G_J]$, and obtain two output results (Subset $G_{I_{unit}}$ of union dictionary G_{unit}, sparse projection vector $\gamma_{I_{unit}}$ of

signal $\boldsymbol{d}_y$ under dictionary $\boldsymbol{G}_{I_{unit}}$). The atoms in $\boldsymbol{G}_{unit}$ can be divided into two groups, one of which is from $\boldsymbol{G}_T$ denoted as $\overline{\boldsymbol{g}}_T^{k_1}, \overline{\boldsymbol{g}}_T^{k_2}, \cdots, \overline{\boldsymbol{g}}_T^{k_j}$, while the other is from $\boldsymbol{G}_J$ denoted as $\overline{\boldsymbol{g}}_J^{k_1}, \overline{\boldsymbol{g}}_J^{k_2}, \cdots, \overline{\boldsymbol{g}}_J^{k_i}$. The coefficient corresponding to $\overline{\boldsymbol{g}}_T^{k_1}, \overline{\boldsymbol{g}}_T^{k_2}, \cdots, \overline{\boldsymbol{g}}_T^{k_j}$ in $\gamma_{I_{unit}}$ is designated as $\gamma_{k_1}, \gamma_{k_2}, \cdots, \gamma_{k_j}$, , and the coefficients corresponding to $\overline{\boldsymbol{g}}_J^{k_1}, \overline{\boldsymbol{g}}_J^{k_2}, \cdots, \overline{\boldsymbol{g}}_J^{k_i}$ in $\gamma_{I_{unit}}$ are $\gamma_{k_{j+1}}, \gamma_{k_{j+2}}, \cdots, \gamma_{k_{j+i}}$.

(3) Select the atom corresponding to $\overline{\boldsymbol{g}}_T^{k_1}, \overline{\boldsymbol{g}}_T^{k_2}, \cdots, \overline{\boldsymbol{g}}_T^{k_j}$ from the dictionary $\boldsymbol{D}_T$ to generate the template $\boldsymbol{R}_T^{k_1}, \boldsymbol{R}_T^{k_2}, \cdots, \boldsymbol{R}_T^{k_j}$, and select the atom corresponding to $\overline{\boldsymbol{g}}_J^{k_1}, \overline{\boldsymbol{g}}_J^{k_2}, \cdots, \overline{\boldsymbol{g}}_J^{k_i}$ from the dictionary $\boldsymbol{D}_J$ to generate the template $\boldsymbol{R}_J^{k_1}, \boldsymbol{R}_J^{k_2}, \cdots, \boldsymbol{R}_J^{k_i}$.

(4) Calculate the approximate autocorrelation matrix of the target and jamming:

$$\widehat{\boldsymbol{R}}_T = \sum_{n=1}^{j} \gamma_{k_n} \boldsymbol{R}_T^{k_n} , \qquad (20)$$

$$\widehat{\boldsymbol{R}}_J = \sum_{n=1}^{i} \gamma_{k_{j+n}} \boldsymbol{R}_J^{k_n} . \qquad (21)$$

(5) Perform eigenvalue decomposition on $\widehat{\boldsymbol{R}}_T$ and $\widehat{\boldsymbol{R}}_J$ to find the approximate Q-KLT basis $\boldsymbol{U}_T^H$ and $\boldsymbol{U}_J^H$ of the target echo and jamming signal.

(6) The basis pursuit algorithm is used to solve the estimate $\boldsymbol{\Theta}_T$ of the sparse representation of the target echo under $\boldsymbol{U}_T^H$, and the estimate $\boldsymbol{\Theta}_J$ of the sparse representation of the jamming signal under $\boldsymbol{U}_J^H$.

(7) Reconstructed to separate target echo $\hat{\boldsymbol{Y}}_T = \boldsymbol{U}_T \boldsymbol{\Theta}_T$, and jamming signal $\hat{\boldsymbol{Y}}_J = \boldsymbol{U}_J \boldsymbol{\Theta}_J$.

IV. SIMULATION RESULTS AND ANALYSIS

A. The simulation results of detection of deception jamming

In this paper, the radar operating at X-band is considered, the time width of LFM signal is 10us, the bandwidth is 10 MHz, PRI=200 us, CPI=64. The number of C&I jamming and SMSP jamming sub-pulses is 20, and the number of repetitions is 5. We assume that the target echo time-delay is 125 us, and the jamming time-delay is 125.5 us. The jamming lag I is 10. The SNR is set to 10 dB and the jamming to signal ratio (JSR) is 30 dB.
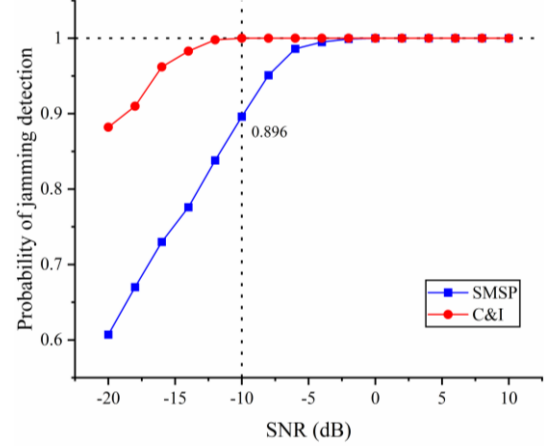
Fig. 4. Detection probability of jamming signal.
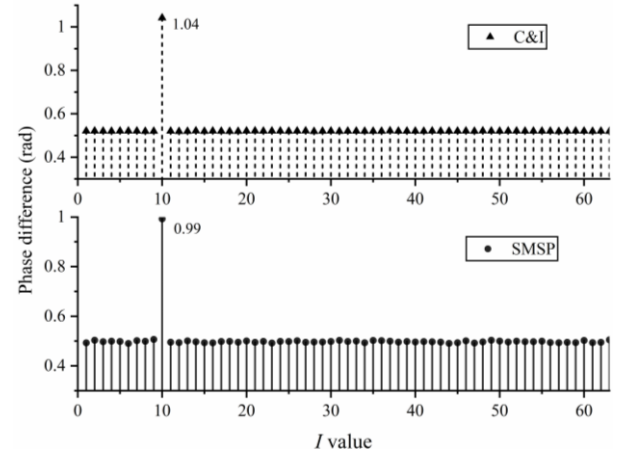
Fig. 5. Estimation of I.

In order to verify the performance of the peak detection method for slice-type interference detection, C&I and SMSP jamming signals are detected by employing the proposed peak detecting method. Figure 4 shows the results of detection probability of jamming signal. It can be seen that as the SNR decreases, the detection probabilities of both jamming signals show a downward trend. Under the same detection threshold, the peak detection method has a higher detection probability for C&I jamming. When SNR=-10 dB, the jamming detection probability remains around 0.9. The simulated results in Fig. 4 demonstrate the effectiveness of the proposed peak detection method for slice-type interference detection.

When the jamming signal is estimated, the number of the period of the signal transmitted by the radar is needed to be determined. Figure 5 is the simulation result of the peak detection method to estimate the lagging I. It can be seen that the corresponding phase difference at

I=10 is twice that of other elements, which shows that for the slice jamming, the peak detection method can effectively estimate the lagging I. The results also can be as the prior information for the anti-jamming method.

B. The simulation results of the optimized design of PPLFM waveform

According to the optimized design of the PPLM waveform, the simulated result is presented in Fig. 6. Figure 6 shows the relevant characteristics of the optimized PPLFM. The code length Q=100 of the phase perturbed term in the PPLFM signal. The GA parameters are set as follows: the maximum number of iterations is 600, the number of populations is 200, the crossover probability is 0.9, and the mutation probability is 0.1. It can be seen from the Fig. 6 that the auto-correlation (AC) and cross-correlation (CC) of the green dotted LFM signal are the same, and the peak of the auto-correlation side-lobe reaches -13.5 dB. The solid blue line represents the auto-correlation of the optimized PPLFM signal. The auto-correlation side-lobe peak reaches -22.18 dB, which is more conducive to the detection of real targets for radar under strong jamming and low SNR conditions.
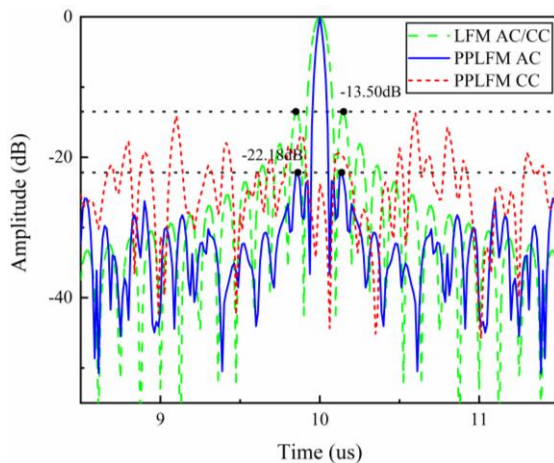
Fig. 6. Related characteristics of PPLFM signals.

C. The simulation results of the dictionary learning method to separate target echo and jamming signal

The effectiveness of the peak detection method is verified under both C&I and SMSP jamming signals in section A. The designed transmitted signal is also given in section B. In this section, the simulation results of the dictionary learning method to separate target echo and jamming signal will be presented.

Figure 7 depicts the results of sliced jamming suppression. The red dotted line represents the result of matched filtering processing of the fixed LFM signal transmitted by the radar. It can be seen that the dense false targets formed by these two sliced jamming completely overwhelm the real targets. In this paper, the agile radar transmits the optimized PPLFM signal, and the solid black line represents the target echo separated by the dictionary learning method. It can be seen that the proposed strategy effectively suppresses the sliced jamming.

(a) C&I

(b) SMSP
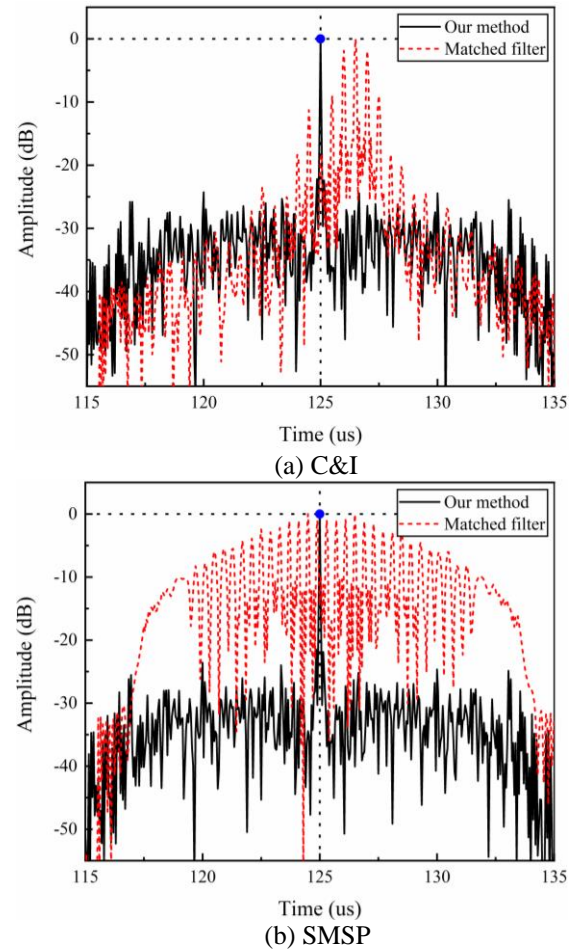
Fig. 7. Suppression results of sliced jamming.

In order to analyze the impact of different JSR and SNR on our strategy to separate signals, we use the gini coefficient to measure the sparsity of the projected vectors of the target and jamming signals under approximate Q-KLT basis. Among them, the gini sparse range is [0, 1], the larger the value, the stronger the sparsity. Figure 8 shows the results of 100 Monte Carlo simulations.

Figure 8 (a) shows that with the improvement of JSR, the sparseness of the target projection vector tends to be stable, and the gini coefficient remains around 0.75. It shows that the sparseness of the projection vector of the target signal under the approximate Q-KLT basis is not affected by the jamming intensity. The sparsity of the target projection vector in Fig. 8 (b)

increases with the increasing of SNR, showing that SNR affects the sparsity of the target projection.

(a) JSR

(b) SNR
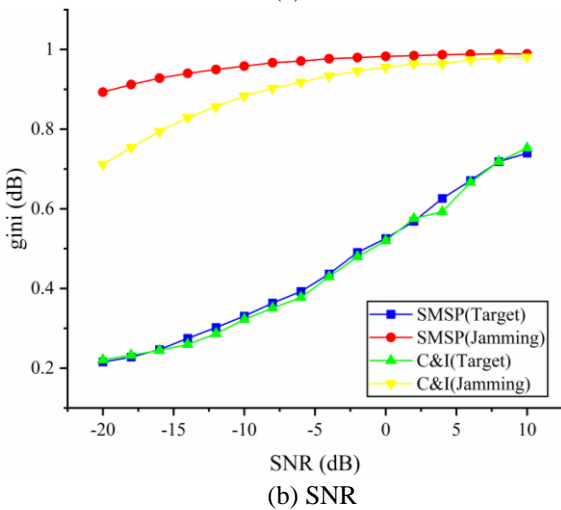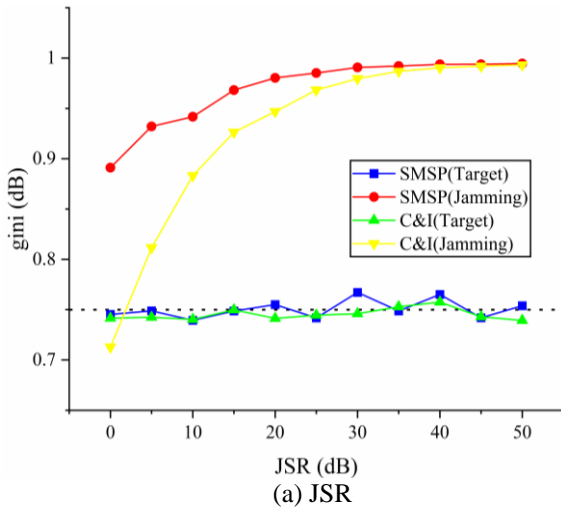
Fig. 8. Gini coefficient versus JSR and SNR.

Next, we evaluate the impact of JSR and SNR on the peak side-lobes ratio (PSLR) after jamming suppression. Figure 9 shows the results of 100 Monte Carlo simulations. Figure 9 (a) shows that the PSLR after this strategy suppresses sliced jamming maintaining around 21.75 dB, which is similar to the gini coefficient of the target projection vector in Fig. 8 (a). Therefore, it is further verified that the PSLR of this strategy is not affected by the jamming intensity. Figure 9 (b) shows that the PSLR decreases as the SNR decreases, and the change trend is still the same as the target gini coefficient change in Fig. 8 (b). And when SNR=-10 dB, the PSLR after interference suppression reaches 18.31 dB, but it shows that the proposed strategy can maintain high anti-jamming performance under low SNR.

Finally, we compare the anti-jamming ability of the proposed strategy with the JBSS method in [10]. Taking SMSP jamming as an example, set JSR=20 dB. We carried out 100 independent trials for Monte-Carlo simulations under the same conditions of other parameters. Figure 10 shows the comparison results of PSLR after jamming suppression for the two methods. It can be seen that the PSLR of the proposed strategy after jamming suppression is better than the JBSS method, and the strategy still maintains good performance under low SNR. The PSLR of the JBSS method drops sharply with the SNR decreases. Since the principle of the JBSS method in [10] is based on the independence between the target and the jamming signal and the correlation between the target signals in different receivers, it will be affected by noise energy. Based on the good sparsity of the PC signals of target and jamming under their respective adaptive dictionaries, these signals can still be well separated under low SNR conditions.

(a) JSR

(b) SNR
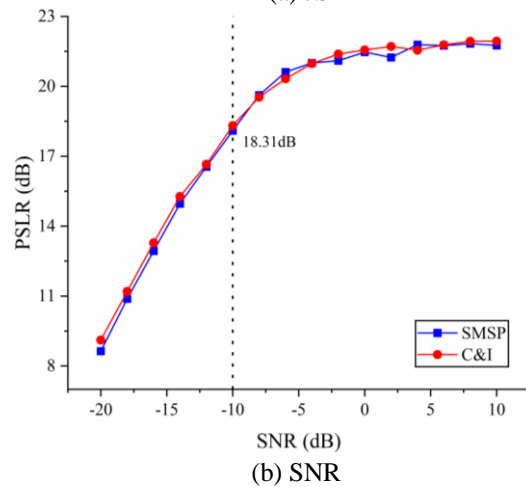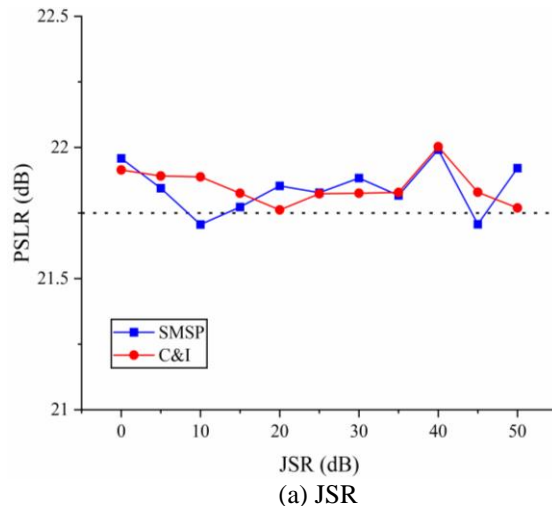
Fig. 9. PSLR after the jamming suppression versus JSR and SNR.
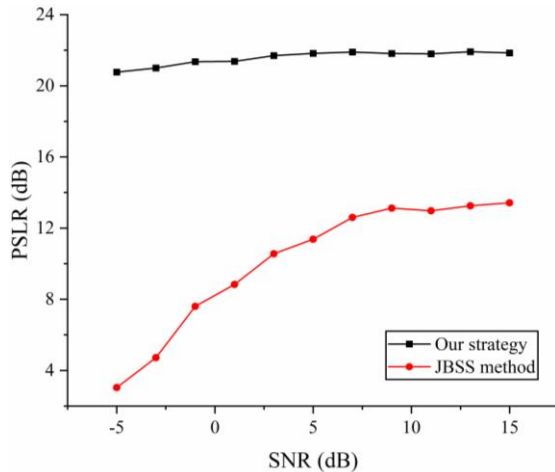
Fig. 10. Performance comparison of the two methods.

V. CONCLUSION

This paper studies the problem of agile LFM radar against dense false target jamming. According to the RPIP signal transmitted by the radar system, we use the peak detection method to detect deception jamming. Then, we construct the target sample set and the jamming sample set, and we implement the separation of the target echo and the jamming signal via the adaptive dictionary learning and the optimized PPLFM signal to achieve the range side-lobes suppression. Finally, simulation experiments are given, the results show that the proposed strategy can effectively detect the presence of jamming and suppress such slice jamming. In addition, the anti-jamming performance is not affected by the jamming intensity. Compared with the JBSS method, it can be concluded that the strategy can still maintain good anti-jamming performance under low SNR conditions. To further improve the performance of the radar, the matched filter can be considered by employing adaptive filter algorithms [13-22] in the future work.

REFERENCES

[1] Q. Shi, N. Tai, C. Wang, and N. Yuan, "On deception jamming for countering LFM radar based on periodic 0-phase modulation," *AEU-International Journal of Electronics and Communications*, vol. 83, pp. 245-252, Jan. 2018.

[2] K. Olivier, J. E. Cilliers, and M. D. Plessis, "Design and performance of wideband DRFM for radar test and evaluation," *Electronics Letters*, vol. 47, no. 14, pp. 824-825, July 2011.

[3] P. Lei, J. Wang, P. Guo, and D. Cai, "Automatic classification of radar targets with micro-motions using entropy segmentation and time-frequency features," *AEU-International Journal of Electronics and Communications*, vol. 65, no. 10, pp. 806-813, Oct. 2011.

[4] N. Tai, H. Han, C. Wang, X. Xu, R. Wu, and Y. Zeng, "An improved multiplication modulation deception jamming method for countering ISAR," *AEU-International Journal of Electronics and Communications*, vol. 110, article number: 152853, Oct. 2019.

[5] G. Lu, S. Liao, S. Luo, and B. Tang, "Cancellation of complicated DRFM range false targets via temporal pulse diversity," *Progress in Electromagnetics Research C*, vol. 16, pp. 69-84, Sept. 2010.

[6] S. Lu, G. Cui, X. Yu, L. Kong, and X. Yang, "Cognitive radar waveform design against signal-dependent modulated jamming," *Progress in Electromagnetics Research B*, vol. 80, pp. 59-77, Mar. 2018.

[7] Z. Liu, J. Sui, Z. Wei, and X. Li, "A sparse-driven anti-velocity deception jamming strategy based on pulse-doppler radar with random pulse initial phases," *Sensors (Basel)*, vol. 18, no. 4, Apr. 2018.

[8] B. Zhou, R. Li, W. Liu, Y. Wang, L. Dai, and Y. Shao, "A BSS-based space-time multi-channel algorithm for complex-jamming suppression," *Digital Signal Processing*, vol. 87, pp. 86-103, Apr. 2019.

[9] Y. Lu, M. Li, R. Cao, Z. Wang, and H. Chen, "Jointing time-frequency distribution and compressed sensing for countering smeared spectrum jamming," *Journal of Electronics and Information Technology*, vol. 38, no. 12, pp. 3275-3281, Dec. 2016.

[10] G. Cui and L. Kong, "Main lobe jamming suppression for distributed radar via joint blind source separation," *IET Radar, Sonar & Navigation*, vol. 13, no. 7, pp. 1189-1199, July 2019.

[11] Y. Li, X. Ying, and B. Tang, "SMSP jamming identification based on Matched Signal transform," *2011 International Conference on Computational Problem-Solving (ICCP)*, Chengdu, China, pp. 182-185, Oct. 21-23, 2011.

[12] A. Aubry, A. D. Maio, M. Piezzo, M. M. Naghsh, M. Soltanalian, and P. Stoica, "Cognitive radar waveform design for spectral coexistence in signal-dependent jamming," *2014 IEEE Radar Conference*, Cincinnati, OH, USA, pp. 0474-0478, May 19-23, 2014.

[13] Y. Li, Z. Jiang, W. Shi, X. Han, and B. Chen, "Blocked maximum correntropy criterion algorithm

for cluster-sparse system identifications," *IEEE Trans. Circuits Syst. II, Express Briefs*, vol. 66, no. 11, pp. 1915-1919, Nov. 2019.

[14] W. Shi, Y. Li, and Y. Wang, "Noise-free maximum correntropy criterion algorithm in non-Gaussian environment," *IEEE Trans. Circuits Syst. II Express Briefs*, vol. 67, no. 10, pp. 2224-2228, Oct. 2020.

[15] W. Shi, Y. Li, and B. Chen, "A separable maximum correntropy adaptive algorithm," *IEEE Trans. Circuits Syst. II, Express Briefs*, vol. 67, no. 11, pp. 2797-2801, Nov. 2020.

[16] Y. Li, Y. Wang, and T. Jiang, "Norm-adaption penalized least mean square/fourth algorithm for sparse channel estimation," *Signal Processing*, vol. 128, pp. 243-251, 2016.

[17] W. Shi, Y. Li, L. Zhao, and X. Liu, "Controllable sparse antenna array for adaptive beamforming," *IEEE Access*, vol. 7, pp. 6412-6423, 2019.

[18] X. Huang, Y. Li, Y. V. Zakharov, Y. Li, and B. Chen, "Affine-projection Lorentzian algorithm for vehicle hands-free echo cancellation," vol. 70, no. 3, pp. 2561-2575, 2021.

[19] T. Liang, Y. Li, W. Xue, Y. Li, and T. Jiang, "Performance and analysis of recursive constrained least Lncosh algorithm under impulsive noises," *IEEE Transactions on Circuits and Systems II: Express Briefs*, vol. 68, no. 7, pp. 2217-2221, 2021.

[20] T. Liang, Y. Li, Y. V. Zakhrow, W. Xue, and J. Qi, "Constrained least Lncosh adaptive filtering algorithm," *Signal Processing*, vol. 183, 2021.

[21] Y. Li and Y. Wang, "Sparse SM-NLMS algorithm based on correntropy criterion," vol. 52, no. 17, pp. 1461-1463, 2016.

[22] Y. Li, C. Zhang, and S. Wang, "Low-complexity non-uniform penalized affine projection algorithm for sparse system identification," *Circuits, Systems, and Signal Processing*, vol. 35, no. 5, pp. 1611-1624, 2016.